Inverse Determination of Temperature-Dependent Thermal Conductivity Using Steady Surface Data on Arbitrary Objects

T. J. Martin
Mem. ASME,
Systems Engineer,
Turbine System & Optimization,
M/S 201-20,
Pratt & Whitney Aircraft Company,
400 Main Street,
East Hartford, CT 06108
e-mail: martinj@pweh.com

G. S. Dulikravich
Fellow ASME,
Professor,
Department of Mechanical and
Aerospace Engineering,
Box 19018,
The University of Texas at Arlington,
Arlington, TX 76019
e-mail: dulikra@mae.uta.edu

An inverse computational method has been developed for the nonintrusive and nondestructive evaluation of the temperature-dependence of thermal conductivity. The methodology is based on an inverse computational procedure that can be used in conjunction with an experiment. Given steady-state heat flux measurements or convection heat transfer coefficients on the surface of the specimen, in addition to a finite number of steady-state surface temperature measurements, the algorithm can predict the variation of thermal conductivity over the entire range of measured temperatures. Thus, this method requires only one temperature probe and one heat flux probe. The thermal conductivity dependence on temperature (k-T curve) can be completely arbitrary, although a priori knowledge of the general form of the k-T curve substantially improves the accuracy of the algorithm. The influence of errors of measured surface temperatures and heat fluxes on the predicted thermal conductivity has been evaluated. It was found that measurement errors of temperature up to five percent standard deviation were not magnified by this inverse procedure, while the effect of errors in measured heat fluxes were even lower. The method is applicable to two-dimensional and three-dimensional solids of arbitrary shape and size. [S0022-1481(00)01703-5]

Keywords: Conduction, Heat Transfer, Inverse, Nonintrusive Diagnostics, Properties

1 Introduction

The ASTM standard for the measurement of heat flux and thermal properties ([1]) mandates the use of a guarded-hot-plate apparatus. This apparatus limits the size and shape of the test specimen to a flat rectangular slab or a rod having circular cross section. Therefore, it cannot be considered to be a nondestructive experimental procedure. The test method may be operated only with one-dimensional heat flow and the specimen conductance is limited to less than 16 $W m^{-2} K$. Errors in the measurements may be caused by deviations from the idealized assembly configuration, heat radiation, temperature gradients in the test specimen, specimen thickness, material inhomogeneity, and material phase change. Compliance with this experimental testing method requires the establishment of a steady-state condition.

These limitations exclude the measurement of thermal conductivity, k, under a variety of circumstances. For example, it may be impractical or even impossible to extract a properly sized and shaped laboratory test specimen out of the given object. In cryogenic materials, it is quite difficult to measure the variation of thermal conductivity particularly because the thermal conductivity versus temperature, $k(T)$, curve is very steep or has inflections in the range of low temperatures. Similarly, thermal conductivity and specific heat are extremely difficult to measure directly within the thin mushy region of a solidifying or melting medium.

It is therefore very desirable to develop a nondestructive evaluation (NDE) technique that can provide information about the temperature-dependence of thermal conductivity. Thermal tomography and inverse thermal design techniques using the boundary element method offer attractive possibilities for these types of problems. Iterative solution procedures with finite differencing or finite element methods are the most often used when solving inverse parameter identification problems ([2–5]). They are often classified as inverse heat conduction problems. Orlande and Ozisik [6] have noted that most work on parameter identification problems has involved the use of finite dimensional minimization techniques. That is, a finite number of interior temperature measurements are taken and the $k(T)$ curve is iteratively modified until the difference between the measured and computed temperatures is minimized in a least-squares fashion. This means that such numerical procedures require intrusive instrumentation.

Algorithms involving an adjoint form of the heat conduction equation have also been used to obtain fairly accurate predictions of thermal conductivities using temperature histories at a single measurement point ([7]). The approach of using unsteady temperature measurements means that there is no need for fairly expensive heat flux probes. On the other hand, the typical inverse methods for determination of $k(T)$ via utilization of the unsteady temperature measurements have not been demonstrated to work on arbitrarily shaped multidimensional objects ([8–11]) and for arbitrary $k(T)$ distributions ([11]).

In this work, we are presenting an inverse numerical procedure that differs substantially from the iterative approaches and from the formulations based on the unsteady temperature measurements. We start by assuming that measured values of steady heat fluxes (or convection heat transfer coefficients) are available everywhere on the surface of an arbitrarily shaped solid. Kirchhoff's transformation ([12]) is then used to convert the governing heat conduction equation into a linear boundary value problem that can be solved for the unknown Kirchhoff's heat functions on the boundary using the boundary element method. Given several boundary temperature measurements, these heat functions are then inverted using numerical differentiation ([13]) to obtain thermal conductivity at the points where the overspecified temperature measurements were taken.

The experimental part of this inverse method requires one thermocouple and one heat flux probe placed sequentially only on the surface of an arbitrarily shaped and sized specimen. Thus, this

Contributed by the Heat Transfer Division for publication in the JOURNAL OF HEAT TRANSFER. Manuscript received by the Heat Transfer Division, April 12, 1999; revision received, February 14, 2000. Associate Technical Editor: A. Majumdar.

method is nonintrusive and directly applicable to field testing since special test specimens do not need to be manufactured. This method could still use steady temperature measurements at isolated interior points if additional accuracy is desired ([14]).

Our inverse method addresses many of the limitations of the guarded-hot-plate experimental test method and offers the ability to overcome most of them. The method is inherently multidimensional and allows for multidirectional temperature gradients in the test specimen. The computer algorithm for the steady-state inverse determination of the temperature variation of thermal conductivity is noniterative (when steady-state boundary heat fluxes and temperatures are provided) and robust, requiring only several seconds on a personal computer.

It should be pointed out that this paper offers a method which is significantly more versatile than our original method ([15]). The present method does not require that experimentally measured surface temperatures must be in equal temperature intervals. The present method also allows that heat transfer coefficients can be used instead of heat flux boundary conditions. The new algorithm also accepts experimentally measured temperatures having same value, but measured at different boundary points.

2 Numerical Formulation

The governing equation for steady-state heat conduction in an isotropic medium with temperature-dependent thermal conductivity is an elliptic quasi-linear partial differential equation,

$$\nabla \cdot [k(T) \nabla T] = 0 \tag{1}$$

This equation can be linearized by the application of Kirchhoff's transformation where the temperature variable, T, can be transformed uniquely to the heat function, $u(T)$,

$$u = \int_0^T \frac{k(T)}{k_0} dT$$

$$\nabla u = \frac{k(T)}{k_0} \nabla T. \tag{2}$$

Kirchhoff's transform converts the governing steady-state heat conduction equation into Laplace's equation, $\nabla^2 u = 0$. Dirichlet boundary conditions can also be transformed by applying Kirchhoff's transformation directly to the boundary temperatures. Neumann boundary conditions can easily be related to the heat flux, Q, in the direction, n, normal to the boundary.

$$Q = -k \frac{\partial T}{\partial n} = k_0 \frac{\partial u}{\partial n} \tag{3}$$

The specification of convective heat transfer coefficients on the boundaries falls into the category of a Robin-type boundary condition. It is a special case of the more general nonlinear heat flux boundary condition, where the heat flux is a function of temperature.

$$Q(T) = -k \frac{\partial T}{\partial n} = h(T - T_\infty) \tag{4}$$

Here, the boundary temperature is a function of the Kirchhoff function, $T = T(u)$. This condition does not pose any difficulties whenever the temperature is overspecified over the entire convective boundary. But, in general, an iterative solution procedure, such as the Newton-Raphson method, will be required. The Robin condition can be made linear by the use of the Jacobian, $\partial Q / \partial u$, of the Kirchhoff transformation.

$$\left(\frac{\partial u}{\partial n}\right)^n = \left(\frac{\partial u}{\partial n}\right)^{n-1} + \frac{1}{k_0} \left(\frac{\partial Q}{\partial u}\right)^{n-1} (u^n - u^{n-1}) \tag{5}$$

Since the thermal conductivity variation is unknown, the iteration must also include the inverse procedure, which will be explained in greater detail in the next section.

To summarize, in the case of Robin boundary conditions, an initial guess to the boundary values of temperature, T, leads to an initial thermal conductivity function, $k(T)$. Given this information, the Jacobian of the transformed nonlinear heat flux boundary condition, $\partial Q / \partial u$, allows for the solution of the field of Kirchhoff functions, $u(T)$.

The inverse procedure uses knowledge of the discrete boundary heat function values, u_i, at the same physical locations where the boundary temperature, T_i, were measured, in order to yield the unknown thermal conductivity curve, $k(T)$. In the case of Robin boundary conditions, this new $k(T)$ curve will produce a heat flux Jacobian that is, in general, different from the initial guess. Therefore, in the case of Robin boundary conditions the aforementioned procedure must be solved iteratively until the heat flux, $Q(T)$, converges to a user-specified tolerance. In most instances, the system of equations is only weakly nonlinear, and the initial thermal conductivity can be a guessed constant. The use of such an iterative procedure allows for the temperature-dependence of the convective heat transfer coefficient, $h(T)$, as well as for any arbitrary temperature-dependent heat flux boundary condition, such as heat radiation. The numerical implementation of this nonlinear methodology for well-posed problems does not produce any serious difficulties ([16]). The implementation of this procedure for the inverse determination of thermal conductivity has yet to be fully investigated.

2.1 Solution to the Direct Problem Using the Boundary Element Method. The boundary element method ([17]) is a powerful computational tool for solving linear and quasi-linear boundary value problems. Its effectiveness in solving inverse problems, such as ill-posed boundary conditions, unknown heat sources, or when temperature measurements are enforced at isolated interior points, has been demonstrated ([18,14]).

In this work, the boundary element method system for steady-state nonlinear heat conduction was written as a system of boundary integral equations ([19]), valid for arbitrary two and three-dimensional geometries. A well-posed (direct or analysis) problem was created when Neumann (or Robin) conditions were provided on all boundaries except for a single boundary point where Dirichlet condition was specified. Integral of all heat fluxes over the entire boundary had to amount to zero. The boundary of the test specimen was discretized with N_{BE} elements connected at their end points with N_{BN} boundary nodes. The variation of u and $\partial u / \partial n$ over each boundary element (line segment) was assumed to be linear. The integration over each boundary element was accomplished using Gaussian quadrature. In the case where a singularity existed at one of the end points of a boundary element, analytic integration was performed. This discretization procedure allowed the nodal quantities of u and $\partial u / \partial n$ to be factored into matrix form, $[\mathbf{H}]\{\mathbf{U}\} = [\mathbf{G}]\{\mathbf{Q}\}$. Thus, the $[\mathbf{H}]$ and $[\mathbf{G}]$ matrices are known because they are strictly dependent upon the Green's function and the geometry.

3 Inverse Method for Determining $k(T)$ Variation

When heat fluxes are known over the entire boundary via steady-state measurements taken on the entire surface of the object, the boundary element method can be used to solve for the transform of the Kirchhoff heat functions on the boundary.

$$[\mathbf{H}]\{\mathbf{U}\} = [\mathbf{G}]\{\mathbf{Q}\} = \{\mathbf{F}\} \tag{6}$$

The matrix $[\mathbf{G}]$ can be multiplied by the vector $\{\mathbf{Q}\}$ to form a vector of known quantities $\{\mathbf{F}\}$ so that the matrix $[\mathbf{H}]$ can be inverted to obtain the values of $\{\mathbf{U}\}$ at each boundary node. The matrix $[\mathbf{H}]$ appears to be well conditioned so that regularization methods are not required. A caution should be exercised since the level of ill-conditioning exhibited by the matrix $[\mathbf{H}]$ could be reduced artificially due to coarse discretization. Since the inversion is nonunique when only Neumann-type (heat flux) boundary conditions are provided everywhere on the boundary, the arbitrary

constant can be determined by specifying at least one Dirichlet boundary condition. Therefore, a modified Kirchhoff transform is required.

$$u = u_1 + \int_{T_1}^{T} \frac{k(T)}{k_0} dT \tag{7}$$

Here, k_0 is a reference conductivity value and T_1 is the minimum value of the measured boundary temperature. The minimum value of Kirchhoff function, $u_{\min}$, occurs at the minimum temperature, $T_{\min}$. Thus, $u_1 = T_1 = T_{\min}$ makes one Dirichlet boundary condition. Then, the boundary element method can be used to obtain the values of the heat function $\{\mathbf{U}\}$ on the entire boundary except at the location of the minimum temperature reading. At this point, the normal derivative $q_1 = (\partial u/\partial n)_1$ will be computed since $T_{\min}$ is specified there.

Now that the nodal boundary values of $\{\mathbf{U}\}$ are known, the entire field of heat functions is known. At any interior point, the values of the Kirchhoff heat function can be obtained in a post-processing fashion. Since the boundary value problem is over-specified, a number of steady temperature measurements, taken either nonintrusively on the boundary, or intrusively, at isolated interior points, can be used to convert the heat functions, $u(T)$, into the corresponding values of thermal conductivity, $k(T)$, at the same physical locations where the measuring instruments were placed. Thus, knowing both vectors $\{\mathbf{U}\}$ and $\{\mathbf{T}\}$, the vector $\{\mathbf{K}\}$ can be determined by performing numerical differentiation of $\{\mathbf{U}\}$. A book by Hansen [13] represents an authoritative text on the general aspects of ill-conditioning and numerical differentiation. For the benefit of general engineering audience we will provide a detailed set of various numerical differentiation procedures that were tested with the objective of finding the most appropriate algorithm for the determination of $k(T)$.

In order to evaluate the sensitivity of the algorithm to errors in the measurement data, random errors based on the Gaussian probability density distribution were added intentionally to the temperature and heat flux measurements. A random number $0 < R < 1$ with a uniform distribution was generated using a standard utility subroutine. The desired variance σ^2 was specified and error was added to the analytic temperature data points, T_{analyt}.

$$T_n = T_{\text{analyt}} \pm \sqrt{-2\sigma^2 \ln R} \tag{8}$$

3.1 Trapezoid Rule for Inverting $u(T)$ Function. Given the value of the computed heat function and the measured temperature at the same point on the boundary, the thermal conductivity can be determined at that point via the inverse Kirchhoff's transform. The integral can be evaluated numerically using the trapezoid rule.

$$u_n = u_1 + \int_{T_1}^{T} \frac{k(T)}{k_0} dT = T_1 + \sum_{n=2}^{N} (T_n - T_{n-1}) \left(\frac{k_n + k_{n-1}}{2k_0} \right) \tag{9}$$

The values of temperature, T_n, are known at a finite number of boundary locations. At these points, the values of the computed heat function, u_n, are also known. Therefore, the values of thermal conductivity, k_n, at these points can be determined using the Kirchhoff's transformation. The inverse of the Kirchhoff's transformation can be expressed as a system of algebraic equations represented in the following matrix form:

$$[\mathbf{C}]\{\mathbf{K}/k_0\} = \{\mathbf{U} - \mathbf{T}_{\min}\} \tag{10}$$

where the elements of the lower-triangular matrix, $[\mathbf{C}]$, have been determined as follows:

$$C_{i1} = \frac{T_2 - T_1}{2} \quad \text{when } j = 1 \tag{11a}$$

$$C_{ii} = \frac{T_j - T_{j-1}}{2} \quad \text{when } i = j \tag{11b}$$

$$C_{ij} = \frac{T_{j+1} - T_{j-1}}{2} \quad \text{when } j < i_{\max}. \tag{11c}$$

By inverting the $[\mathbf{C}]$ matrix, the values of the thermal conductivity can be obtained at the same locations where the temperature measurements were taken. The values of the temperature must be sorted in ascending order $\{T_1, T_2, \ldots, T_N\}$ and identical temperature readings must be discarded. This system represents $N-1$ equations for N unknowns. The additional equation arises from the knowledge of the conductivity at the minimum temperature point. At this point both the heat flux, $Q|_{T_{\min}}$, and the normal derivative of the heat function, $k_0(\partial u/\partial n)|_{u_{\min}} = k(\partial T/\partial n)|_{T_{\min}}$ are known from the boundary element method solution.

The trapezoid rule provided good results, but the predicted values of the thermal conductivity were often oscillatory. Simpson's rule was attempted to remove this oscillatory behavior and it was successful at doing this, but the $k(T)$ curve that it predicted was often incorrect at the endpoints of the measured temperature range. Instead, very good results were obtained by simply averaging the results predicted by the trapezoid rule.

Regularization was required to properly invert the $[\mathbf{C}]$ matrix whenever random error was introduced into the temperature measurements. Tikhonov's regularization ([20]) is a single-parameter minimization where the solution vector $\{\mathbf{K}/k_0\}$ minimizes the weighted sum of the norm of the error vector. A minimum error norm was found by differentiating Eq. (10) with respect to each component of the unknown vector $\{\mathbf{K}/k_0\}$ and setting the result equal to zero. Substituting the singular value decomposition where $[\mathbf{C}] = [\mathbf{E}][\mathbf{W}][\mathbf{D}]$ ([21–22]) and solving for the unknown vector $\{\mathbf{K}\}$ resulted in

$$\frac{1}{k_0}\{\mathbf{K}\} = [\mathbf{E}]([\mathbf{W}]^T[\mathbf{W}] + \lambda[\mathbf{I}])^{-1}[\mathbf{W}]^T[\mathbf{D}](1 - T_{\min})\{\mathbf{U}\} \tag{12}$$

where $[\mathbf{I}]$ is the identity matrix. Tikhonov's regularization is a generalization of least-squares truncation, but instead of simply eliminating terms associated with small singular values, they are weighted by a factor $(1 + \lambda/w^2)$, where w are the eigenvalues of matrix $[\mathbf{C}]$. Larger regularization parameters, λ, had the effect of increased smoothing of the $k(T)$ curve without adding error into the solution of the heat conduction equation ([18]).

A similar regularization procedure ([23,13]) provided even greater smoothing of the predicted $k(T)$ function with the addition of a smoothing matrix $[\mathbf{S}]$.

$$\frac{1}{k_0}\{\mathbf{K}\} = [[\mathbf{C}]^T[\mathbf{C}] + \gamma[\mathbf{S}]]^{-1}[\mathbf{C}]^T(1 - T_{\min})\{\mathbf{U}\} \tag{13}$$

The smoothing parameter, γ, was increased with the increased amount of error in the temperature and/or heat flux boundary conditions. The optimal magnitude of γ was proportional to the square of the error in temperature.

3.2 Finite Differentiation for Inverting $u(T)$ Function. As an alternative method, the nodal quantities of $\{\mathbf{U}\}$ and $\{\mathbf{T}\}$ were easily converted into values of thermal conductivity $\{\mathbf{K}\}$ using finite difference formulas. Second and third-order accurate finite difference formulas for thermal conductivity, $k_{i,2}$ and $k_{i,3}$, respectively, were used with irregular temperature intervals. Thus,

$$k_{i,2} = \frac{\delta_{u1}}{\delta_{T1}} \tag{14}$$

$$k_{i,3} = \frac{\delta_{u1}\delta_{T_2}^2 - \delta_{u2}\delta_{T1}^2}{\delta_{T2}\delta_{T3}} \tag{15}$$

where

$$\delta_{u1}=u_{i+1}(T_i-T_{i-1})^2-u_i[(T_i-T_{i-1})^2-(T_{i+1}-T_i)^2]-u_{i-1}(T_{i+1}-T_i)^2 \quad (16a)$$

$$\delta_{u2}=u_{i+2}(T_i-T_{i-2})^2-u_i[(T_i-T_{i-2})^2-(T_{i+2}-T_i)^2]-u_{i-1}(T_{i+2}-T_i)^2 \quad (16b)$$

$$\delta_{T1}=(T_{i+1}-T_i)(T_i-T_{i-1})(T_{i+1}-T_{i-1}) \quad (16c)$$

$$\delta_{T2}=\delta_{T1}(T_{i+2}-T_i)(T_i-T_{i-2})(T_{i+2}-T_{i-2}) \quad (16d)$$

$$\delta_{T3}=[(T_{i+2}-T_i)(T_i-T_{i-2})-(T_{i+1}-T_i)(T_i-T_{i-1})] \quad (16e)$$

$$\delta_{T1}^2=(T_{i+1}-T_i)^2(T_i-T_{i-1})^2(T_{i+1}-T_{i-1}) \quad (16f)$$

$$\delta_{T2}^2=(T_{i+2}-T_i)^2(T_i-T_{i-2})^2(T_{i+2}-T_{i-2}). \quad (16g)$$

Here, $k_{i,2}$ and $k_{i,3}$ are the thermal conductivities obtained at the ith boundary node with the second and third-order differencing formulas, respectively. These finite difference formulas gave satisfactory results for $k(T)$ whenever the errors in the temperature measurements were small. The use of finite differencing method required the discarding of temperature readings that were within the error bounds of the temperature readings.

3.3 Linear Least Squares for Inverting $u(T)$ Function. In an effort to improve the inverse procedure, as well as to utilize an a priori knowledge about the general shape of thermal conductivity function, $k(T)$, a general linear least-squares algorithm ([21,22]) was employed. The objective of this approach was to fit the set of N data points $[T_n, u_n]$ to a selected mathematical model. The general linear least-squares model used a linear combination of M basis functions.

$$u(T)=\sum_{m=1}^{M} c_m P_m(T) \quad (17)$$

where $P_1(T)$, $P_2(T)$, . . . ,$P_M(T)$ are arbitrary fixed nonlinear functions of temperature, called the basis functions. The merit function, called chi-squared, χ^2, is a measure of how well the models fit the data. It assumes that the measurement errors are supplied as standard deviations, σ_1, of the temperature. Then,

$$\chi^2=\sum_{n=1}^{N}\left[\frac{u_i-\sum_{m=1}^{M} c_m P_m(T_n)}{\sigma_n}\right]. \quad (18)$$

The minimum of this function occurs where the derivative of χ^2 with respect to all M basis function coefficients, c_m, vanishes. The resulting system of equations was cast into the following covariance matrix formulation:

$$\left[\sum_{n=1}^{N}\frac{P_i(T_n)P_j(T_n)}{\sigma_n^2}\right]\{\mathbf{c}_j\}=\left\{\sum_{n=1}^{N}\frac{u_n P_i(T_n)}{\sigma_n^2}\right\}. \quad (19)$$

Here, {c} is the vector of unknown basis function coefficients. The inversion of the covariance matrix with Gaussian elimination or the SVD algorithm ([21,22]) yielded the basis function coefficients. Knowing these coefficients, the basis functions were differentiated with respect to temperature in order to obtain the values of thermal conductivity, k_n, at the N data points.

The challenge here was to select an appropriate set of the basis functions that best modeled the integral of the thermal conductivity function. In this paper, several basis functions were attempted; standard polynomials, Chebyshev polynomials, and third-order beta-splines ([24]), in addition to nonarbitrary basis functions in which a priori knowledge of the $k(T)$ curve was assumed. In the latter case, for example, arctangent integral basis functions were used to estimate a step-like $k(T)$ variation. These basis functions were integrated either analytically or numerically. We also tried using Fourier sine and cosine series basis functions, but the results were less than satisfactory, with large oscillations increasing with increasing input error.

3.3.1 Polynomial Basis Functions. The thermal conductivity was represented by a standard series of polynomial basis functions.

$$k(T)=c_1+c_2T+c_3T^2+\ \ldots\ +c_MT^{M-1} \quad (20)$$

The Kirchhoff function, $u(T)$, was obtained by analytical indefinite integration of these polynomials with respect to temperature, thereby yielding an additional basis function coefficient, c_0. The general linear least-squares algorithm then determined the unknown coefficients, $c_0, c_1, \ldots, c_M$.

3.3.2 Chebyshev Basis Functions. The thermal conductivity variation was represented by the series of orthogonal Chebyshev functions,

$$k(T)=\sum_{m=0}^{M} c_m \cos(m \arccos(\theta)), \quad (21)$$

where the temperature was affected by a change of variable.

$$\theta=\frac{T-(T_{\min}+T_{\max})/2}{(T_{\max}-T_{\min})/2} \quad (22)$$

In order to use these functions to approximate the $u(T)$ data, the Chebyshev basis functions were integrated numerically. When the explicit polynomial expressions were used instead of the trigonometric functions, the basis functions were integrated analytically. The general linear least-squares algorithm then determined the coefficients of the integrated Chebyshev basis functions.

3.3.3 Beta-Spline Basis Functions. The Kirchhoff function was represented by a piecewise beta-spline of cubic polynomial segments, $b_k(s)$.

$$u(T)=\sum_{i=1}^{N_{\text{vert}}}\left[\sum_{k=-1}^{3} b_k(\beta_1,\beta_2,s)V_{i+k}\right] \quad (23)$$

Each segment was regarded as a weighted average of its four local vertices, so that each segment was a function of the parameter $s(T)$ in a nondimensional curve-following coordinate system that varied from 0 at the beginning of the segment to 1 at the end of that segment.

$$s(T)=1+\frac{T-T_{\min}}{T_{\max}-T_{\min}}(N_{\text{vert}}-1)-\text{int}\left\{1+\frac{T-T_{\min}}{T_{\max}-T_{\min}}(N_{\text{vert}}-1)\right\} \quad (24)$$

Here, the int{ } function also defines the truncated integer value of its argument. V_{i+k} are the control vertex coordinates and $b_k(\beta_1,\beta_2,s)$ are the basis functions. Given a temperature T, the local beta-spline was controlled by the $i-1$ to $i+2$ vertices, where the index i was determined from the above integer truncation. Each basis function was itself described as a cubic polynomial.

$$b_k(\beta_1,\beta_2,s)=\sum_{j=0}^{3} c_{j,k}(\beta_1,\beta_2)s^j \quad (25)$$

The unknown constants $c_{j,k}(\beta_1,\beta_2)$ were fixed quantities, provided β_1 and β_2 were fixed. They were found by imposing the three connectivity boundary conditions on any two neighboring segments ([24]). The shape parameter β_1 is referred to as the bias parameter. It could produce clustering towards the end vertices. The second parameter, β_2, is called the tension parameter, and it was always positive. For high values of β_2, the curve is strongly pulled toward the control vertices and, in the limit as $\beta_2\to\infty$, the

beta-spline is identical to the control polygon. The least-squares fitting algorithm ([22]) determined the beta-spline control vertices as basis function coefficients. The thermal conductivity function was then determined by numerically differentiating the piecewise spline with respect to the temperature.

In an alternative approach, the $k(T)$ curve was modeled with the beta-spline, while the Kirchhoff function, $u(T)$, was evaluated as the integral of it.

$$u(T)=\frac{1}{k_0}\int_0^T \sum_{i=1}^{N_{\text{vert}}}\left[\sum_{k=-1}^{3} b_k(\beta_1,\beta_2,s)V_{i+k}\right]dT+c_0 \quad (26)$$

In both cases, the beta-spline curve was either numerically differentiated or numerically integrated. When using the differentiated beta-spline, the basis function coefficients influenced only a local portion of the $k(T)$ curve between the $i-1$ to $i+2$ control vertices. When the integrated beta-spline was used, each basis function coefficient affected the $u(T)$ curve from the beginning of the curve ($T=T_{\min}$) up to the local temperature, T.

4 Numerical Results

All of the above-mentioned methods have been programmed and tested on a simple two-dimensional specimen and an unconventionally shaped two-dimensional specimen. The general formulation of this inverse methodology is also applicable to arbitrary three-dimensional objects.

4.1 Results for a Rectangular Plate. Although the inverse boundary element method approach with the Kirchhoff's transform is directly applicable to arbitrary three-dimensional problems, for the sake of simplicity it will be demonstrated on a two-dimensional geometry. A rectangular plate test specimen 10-cm wide by 1-cm long was used. The opposite ends of the plate were

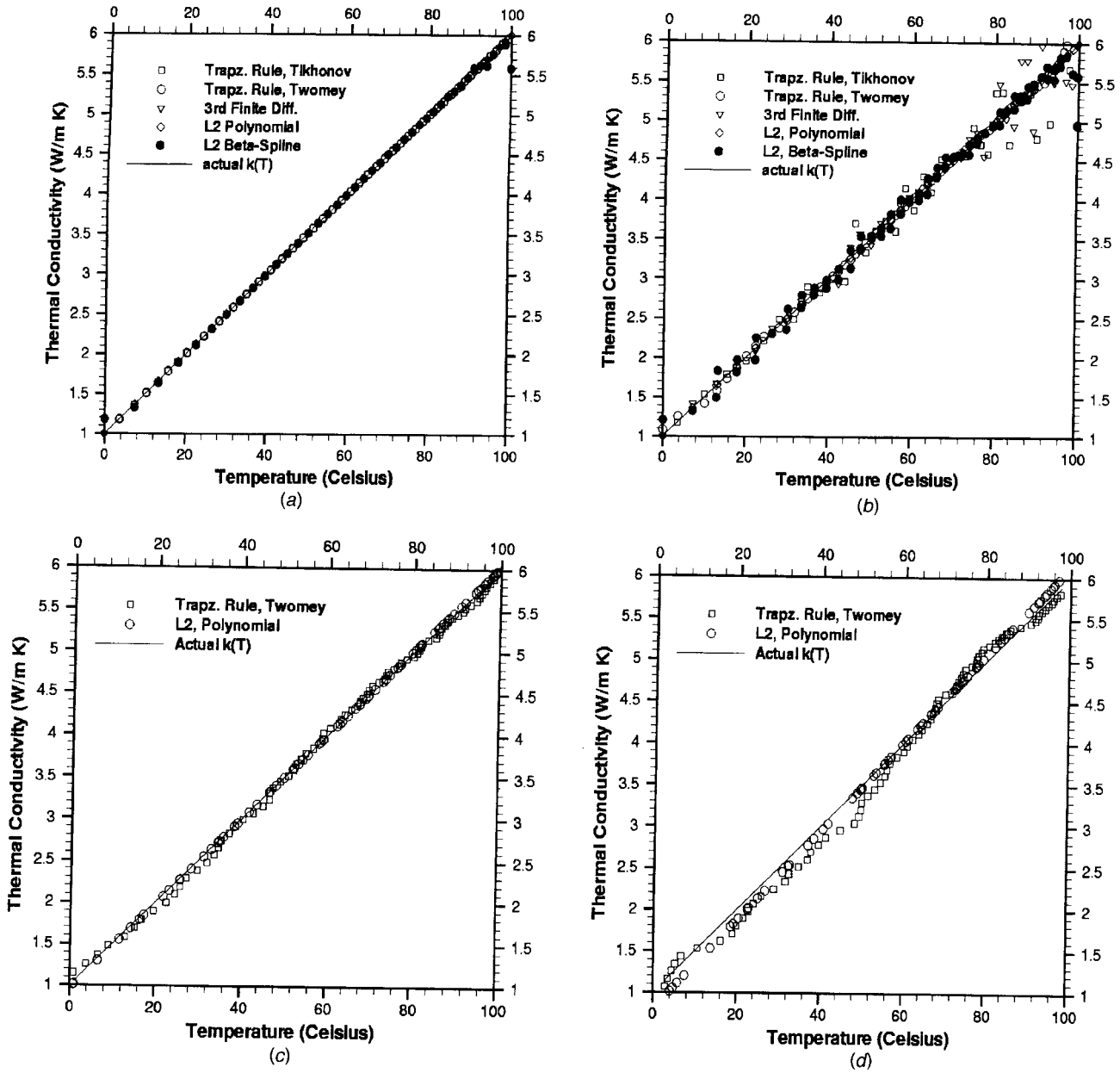

Fig. 1 Variation of the thermal conductivity versus temperature for various amounts of input error in temperature (*a*) $\sigma=0.0°C$, (*b*) $\sigma=0.1°C$, (*c*) $\sigma=1.0°C$, and (*d*) $\sigma=5.0°C$. The inverse boundary element method results are compared to the actual linear conductivity versus temperature function, where $\beta=0.05°C^{-1}$, $T_0=0.0°C$, and $k_0=1.0\,W\,m^{-1}°C$.

kept at constant temperatures of 100.0°C and 0.0°C, respectively. The long side walls were considered to be adiabatic.

When the conductivity versus temperature was a linear function,

$$k(T)=k_0(1+\beta(T-T_0)), \tag{27}$$

the temperatures and heat fluxes can be found from an analytic solution ([25]),

$$\frac{\beta}{2}T^2+T=\left(T_{\text{hot}}+\frac{\beta}{2}T_{\text{hot}}^2\right)-\left(1+\frac{\beta}{2}(T_{\text{hot}}+T_{\text{cold}})\right)$$

$$\times\frac{(z_{\text{hot}}-z_{\text{cold}})}{(z_{\text{cold}}-z_{\text{hot}})}(T_{\text{hot}}-T_{\text{cold}}). \tag{28}$$

For the computational analysis, each of the long sides of the specimen was discretized with 40 equal-length linear isoparametric boundary elements. Only four such elements were used on each of the two short sides. In the case of an actual experimental evaluation of the surface heat fluxes this means that a single heat flux probe was applied at a total of 88 locations corresponding to the midpoints of the 88 boundary elements. The forward boundary element method solution compared very well with the analytic solution, averaging an error of less than 0.1 percent for a wide range of the parameter β ([14]).

4.1.1 Linear Variation of Thermal Conductivity. The actual variation of thermal conductivity versus temperature was linear between the values of $k(T=0°C)=1.0\,\text{Wm}^{-1}°\text{C}$ and $k(T=100.0°C)=6.0\,\text{Wm}^{-1}°\text{C}$. The top and bottom walls of the rectangular plate were specified to be adiabatic. The right and left end walls were specified with the heat flux taken from the analytic solution ($Q=\pm 35.0\,\text{Wm}^{-2}$), except for the center of the right side at which a single temperature measurement was specified, T_{min}.

The boundary element method computed the Kirchhoff's heat functions at each of the boundary nodes. These heat functions were inverted into values of thermal conductivity at the nodes where the overspecified temperature measurements were provided. These temperatures existed at discrete locations along the adiabatic long sides of the specimen.

Figure 1 shows the predicted values of thermal conductivity versus temperature using various procedures for inverting the $u(T)$ function. Errors in the temperature measurements were simulated by adding standard deviations of 0.1°C up to 5.0°C (0.1 percent to 5.0 percent). All of the inverse methods had very good accuracy whenever the errors were less than 1.0 percent. For errors above 1.0 percent, only the Twomey regularization procedure and the linear least squares with polynomial basis functions were accurate enough. The beta-spline basis functions were not used on this example. The magnitude of the optimum Twomey regularization parameter, γ, was proportional to the square of the average temperature. The Chebyshev polynomial and beta-spline methods had problems at the endpoints due to their oscillatory nature. The linear least-squares with polynomial basis functions were the most accurate because the actual conductivity and Kirchhoff functions were represented by polynomials.

4.1.2 Errors in the Heat Flux Boundary Conditions. The inverse procedure was also evaluated given errors in the measured heat fluxes. The behavior of the inverse algorithm on the same rectangular test specimen with linear temperature-dependence of thermal conductivity was observed with intentionally introduced errors in the measured heat fluxes of 1.0 percent, 5.0 percent, and 10.0 percent. It is remarkable that the inverse algorithm is less sensitive to errors in the measured heat fluxes (Fig. 2) than in the measured temperatures. This was because heat fluxes were applied as boundary conditions to the boundary element method, and the Laplacian operator smoothed errors in these heat fluxes. On the other hand, errors in the measured temperatures directly affect the results of the inverse procedure.

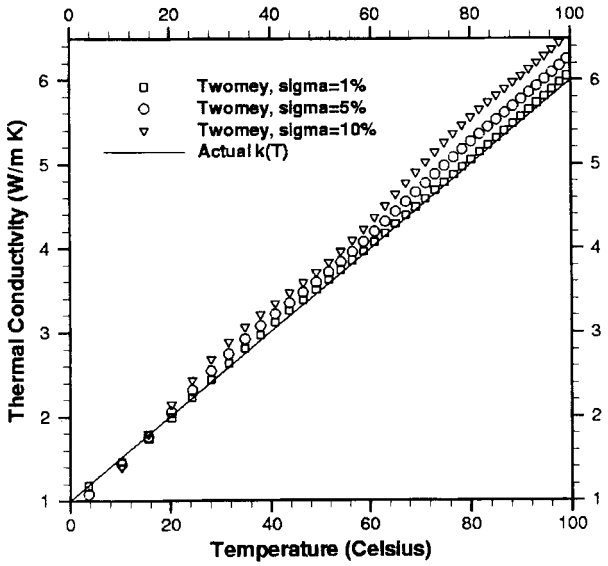

Fig. 2 Predicted temperature-dependence of thermal conductivity when errors were added to the heat fluxes compared to the actual linear variation of $k(T)$

It is noticeable that the predicted thermal conductivity values are somewhat biased towards the hot end of the test specimen (Fig. 2). This was most likely due to the fact that the only Dirichlet (temperature) boundary condition was specified on the cold end. This confirms our earlier observations ([18]) that the farthest point from the overspecified temperature boundary condition has the greatest amount of bias in the predicted temperature and, subsequently, thermal conductivity.

4.1.3 Steep Jump Variation of Thermal Conductivity. Next, the actual variation of thermal conductivity versus temperature was described by the arctangent function.

$$k(T)=\frac{1}{2}(1-\xi)k_{\text{min}}+\frac{1}{2}(1+\xi)k_{\text{max}}$$

$$\xi=\frac{k_{\text{max}}-k_{\text{min}}}{2\pi}\arctan\left(\alpha\frac{(T_{\text{max}}+T_{\text{min}})}{2}\right) \tag{29}$$

Here, α is a parameter that sets the slope of the jump in the k-T curve. The top and bottom walls of the rectangular plate were specified to be adiabatic and the right and left walls were specified with the heat flux taken from the well-posed boundary element method solution ($Q=\pm 15.0\,\text{Wm}^{-2}$). The boundary temperatures were taken from the well-posed boundary element method solution and prescribed to the inverse program with varying degrees of error ($\sigma=0.0$, 0.1°C, 1.0°C, and 5.0°C). Figure 3 shows the computed k-T curves when the Tikhonov, Twomey, and finite differencing inverse methods were used. Again with these methods, the results were good when the input temperature measurements have errors with a standard deviation of less than 0.5°C.

Figure 4 shows the results of the linear least-squares algorithm whenever polynomial, arctangent, and Chebyshev basis functions were used. Notice that the use of arctangent basis functions produced very accurate results, indicative of the advantage of having at least some a priori knowledge of the $k(T)$ function shape. The oscillatory behavior of the polynomial and Chebyshev basis functions is evident in these figures, but the general nature of the $k(T)$ curve was captured.

Beta splines were also used with the least squares in an attempt to reduce the severity of these oscillations. Figure 5 presents the results when using the beta-spline basis functions. Here, the beta-spline was used to approximate the $u(T)$ curve so that the thermal

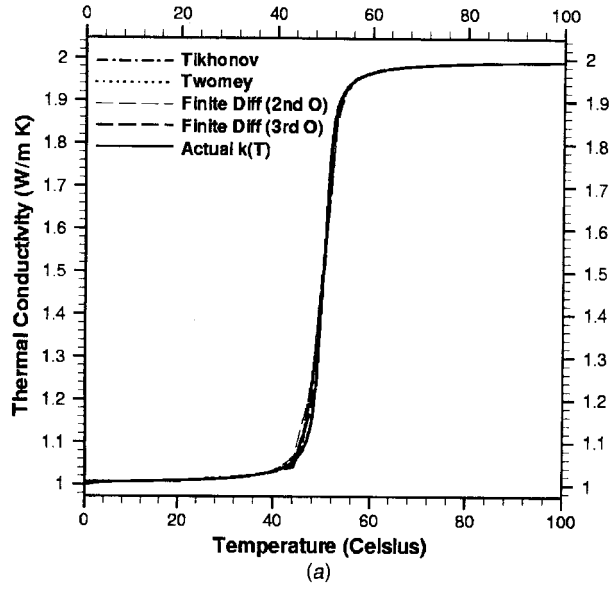

Fig. 3 Variation of the thermal conductivity versus temperature for various levels of input error in temperature, (*a*): $\sigma = 0.0°C$, and (*b*): $\sigma = 0.5°C$. The boundary element method results are compared to the actual arctangent conductivity versus temperature function when $\delta = 1.0°C^{-1}$.

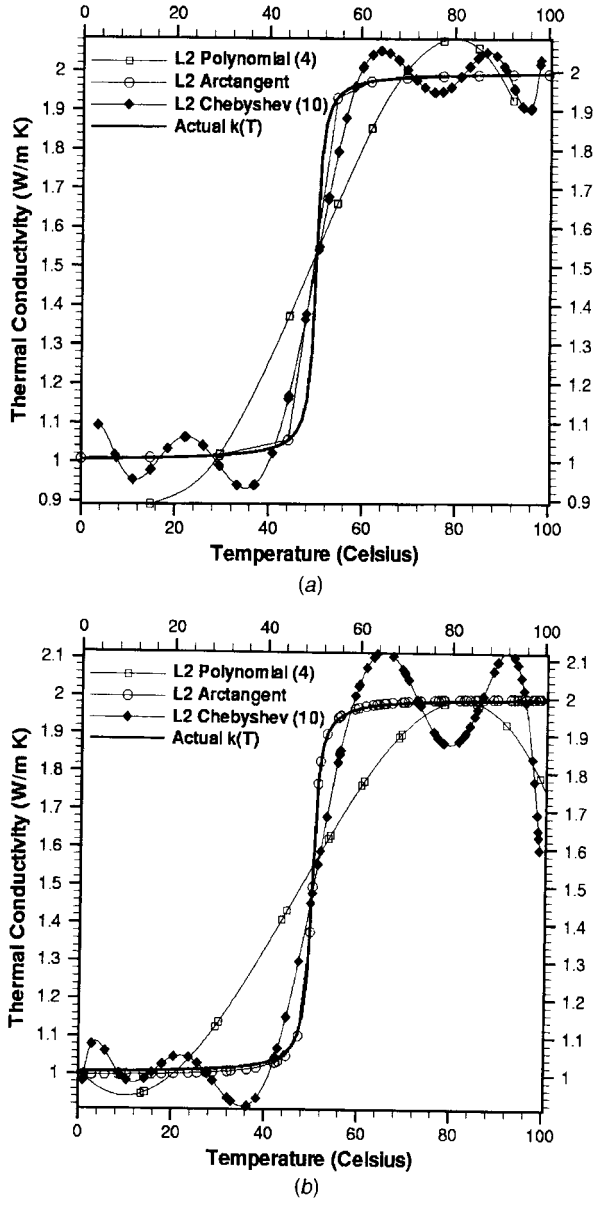

Fig. 4 Variation of the thermal conductivity versus temperature for various levels of input error in temperature, (*a*): $\sigma = 1.0°C$, and (*b*): $\sigma = 5.0°C$. The inverse boundary element method results are compared to the actual arctangent conductivity versus temperature function when $\delta = 1.0°C^{-1}$.

conductivity was numerically differentiated. The oscillations were somewhat suppressed at low input errors, but they became worse with input errors above 1.0 percent. Although more beta-spline vertices produced more accurate representations of the $k(T)$ curve at low input error, the reduction in the number of beta-spline vertices was needed at higher input errors because the oscillatory behavior of the beta-splines needed to be reduced. Consequently, the number of beta-spline vertices had to be reduced from 48 with no input error, down to six vertices for the cases with 5.0 percent input error.

As an alternative, the option of fitting the integrated beta-spline slightly improved the results. This improvement was probably due to the fact that the coefficients of the integrated beta-spline had a more global impact on the least squares objective. Figure 6 demonstrates the ability of the inverse formulation to capture a steep jump in thermal conductivity with the integrated beta splines.

4.2 Inverse Determination of Thermal Conductivity of Copper at Low Temperatures. Thermal conductivity reaches very high values at very low temperatures because the lattice waves are harmonic and can be superimposed without mutual interference. There, the lattice thermal conductivity of crystals depends upon the grain size. As the temperature increases, the lattice vibrations become nonharmonic, scattering is increased, and the thermal conductivity decreases sharply. In metals, heat is predominantly transported by valence electrons rather than by the lattice vibrations, but the effect is the same. The electronic component of thermal conductivity is dependent upon the scale of the impurities rather than upon the crystal grain size and, in pure metals, is one to two orders of magnitude larger than the lattice conductivity. The thermal conductivity decreases sharply beyond 10.0 K primarily because electrons are scattered by thermal vibrations in the lattice.

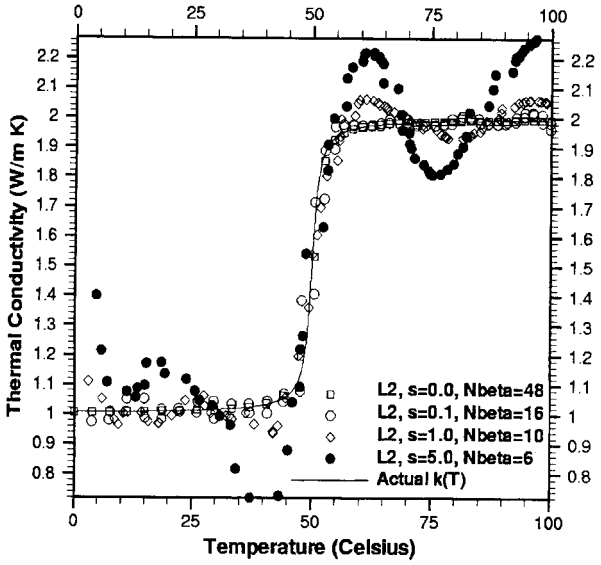

Fig. 5 Variation of thermal conductivity versus temperature predicted with the beta-spline basis functions. The inverse boundary element method results are compared to the actual arctangent conductivity versus temperature function when $\delta = 1.0°C^{-1}$.

Our inverse boundary element method algorithm was attempted on a real material, copper, in the range of very low temperatures to see if the temperature-dependency of thermal conductivity can be determined where there are steep gradients in the $k(T)$ function. The actual temperature-dependency was taken from the *Journal of Physical and Chemical Reference Data* ([26]). The test specimen had the same geometry and grid specifications as in the previous examples.

When there was no error intentionally added to the temperature measurements, the results of the inverse procedure were very accurate for the methodologies used (Fig. 7(*a*)). The finite differencing and the least squares algorithm with beta-spline basis func-

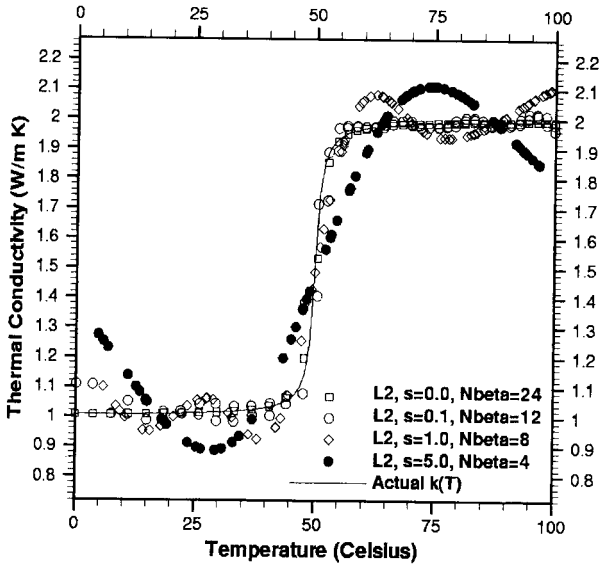

Fig. 6 Variation of thermal conductivity versus temperature predicted with the integrated beta-spline basis functions. The inverse boundary element method results are compared to the actual arctangent conductivity versus temperature function when $\delta = 1.0°C^{-1}$.

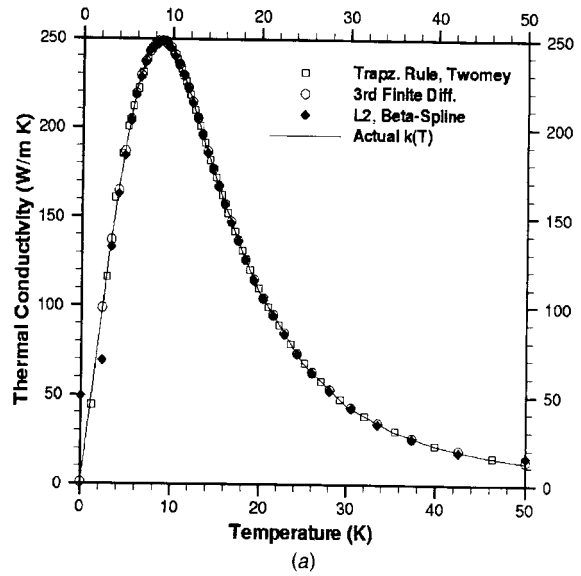

(*a*)

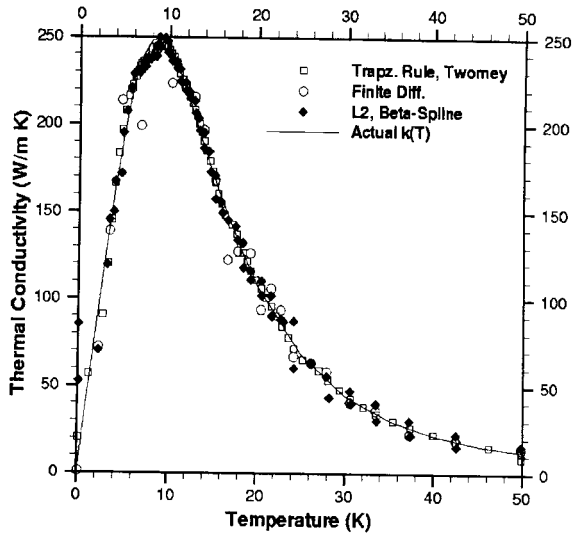

(*b*)

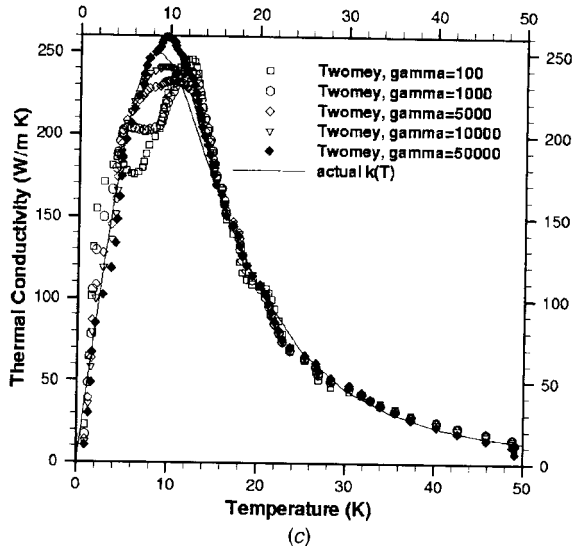

(*c*)

Fig. 7 Inverse determination of the thermal conductivity of copper in the cryogenic range. The best inverse results are shown with various levels of input error:(*a*) $\sigma = 0.0$ K, (*b*) $\sigma = 0.1$ K, and (*c*) $\sigma = 1.0$ K.

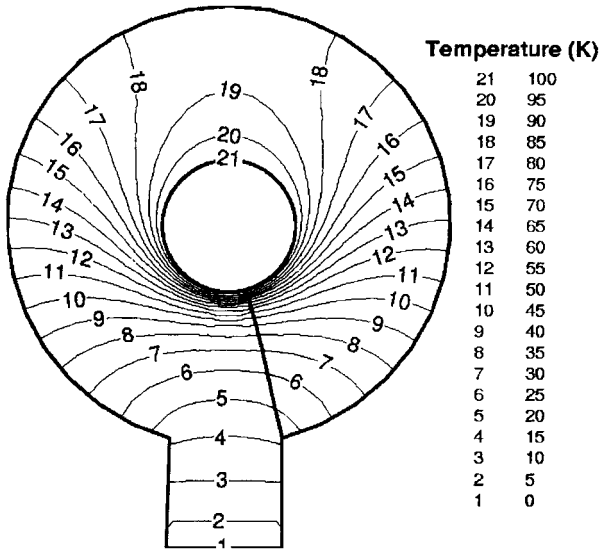

Fig. 8 Temperature contours predicted by nonlinear boundary element method within an arbitrarily shape specimen that was internally heated and made of copper (*b*)

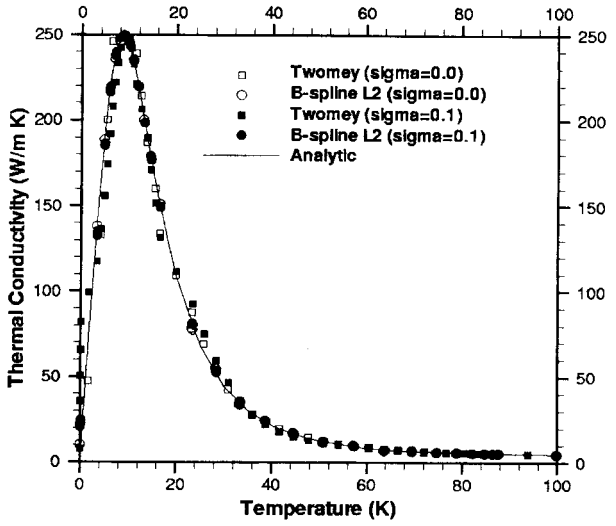

Fig. 9 Inverse prediction of thermal conductivity variation of an arbitrarily shaped specimen made of copper

tions had greater difficulty in capturing the curve once the errors were increased much beyond 0.1 K. The Twomey regularization procedure stayed effective beyond errors of 1.0 K. Figure 7(*c*) demonstrates that the accuracy of the solution is affected by the magnitude of the regularization parameter. The best result existed at very high values of γ, and also where the k-T curve was the smoothest, that is, where the integrated function, dk/dT, was at the first local minimum.

4.3 Applicability to Arbitrary Shapes. To demonstrate the applicability of the general inverse methodology to specimens of arbitrary shapes, we developed the geometry shown in Fig. 8. This object was assumed to be made of a homogenous material with an internally heated cylindrical core and an attachment (bottom surface) kept at a very cold temperature. The forward (direct) boundary element method heat conduction algorithm solved for the temperature field in the object such that the internal circular boundary was held at a constant temperature of 100.0 K and the bottom of the cold attachment was held at a constant temperature of 0.0 K. All other boundaries were assumed to be adiabatic. Figure 8 shows the predicted isotherms in the object made of copper.

Next, the material of the object was assumed to be unknown. The temperatures predicted on the outer (adiabatic) circular boundary by the forward boundary element method were applied as the overspecified boundary conditions for the inverse thermal conductivity problem. Only temperatures were assumed known on the inner circular boundary and the bottom of the attachment. Twomey smoothing was used to invert the coefficient matrix arising from the trapezoid rule. The β-spline was used as the alternative method with 16 vertices computed as the unknown coefficients of the least-squares method. The inversely predicted thermal conductivity variations with temperature are shown in Fig. 9. This figure shows results with and without intentionally introduced errors in the boundary temperature data. Notice that the inverse prediction of the $k(T)$ is very good over the entire range of measured temperatures for this doubly connected two-dimensional object.

5 Conclusions

An inverse computational procedure has been developed to predict the unknown temperature variation of thermal conductivity for arbitrarily shaped test specimens. The procedure is entirely nonintrusive and nondestructive, relying only upon boundary measurements. It is fast and accurate, requiring the knowledge of overspecified steady-state temperature and heat flux or heat transfer coefficients over at least a portion of the boundary. The boundary element method was used to determine the field of the Kirchhoff transform function and its inversion yielded values of thermal conductivity at the locations and temperatures of the instrument readings. Several different inversion procedures were attempted, including regularization, finite differencing, and least-squares fitting with basis functions. The program was very accurate when the data was without error. For most of the inversion procedures it did not excessively amplify input temperature measurement errors when those errors were less than one to five percent standard deviation. The program was found to be less sensitive to measurement errors in heat fluxes than to errors in temperatures. The accuracy of the algorithm was greatly increased with the use of a priori knowledge about the thermal conductivity basis functions. One computational solution required only several seconds on a personal computer.

Acknowledgments

The authors are grateful for the NASA-Penn State Space Propulsion Engineering Center Graduate Student Fellowship facilitated by Prof. Charles Merkle, the National Science Foundation Grant DMI-9522854 monitored by Dr. George Hazelrigg, the NASA Lewis Research Center Grant NAG3-1995 facilitated by Dr. John Lytle and administered by Dr. Cestutis Civinskas, and for ALCOA Foundation Faculty Fellowship administered by Dr. Yimin Ruan.

Nomenclature

F = objective function
$[\mathbf{G}]$ = geometric coefficient matrix
$[\mathbf{H}]$ = geometric coefficient matrix
h = thermal convection coefficient
k = thermal conductivity
Q = heat flux
q = Kirchhoff's heat flux
$\{\mathbf{Q}\}$ = vector of Kirchhoff's heat fluxes
R = random number
T = temperature
u = Kirchhoff's heat function
$\{\mathbf{U}\}$ = vector of Kirchhoff's heat functions
z = coordinate

Greek Letters

α = coefficient of steepness of k-T curve
β = coefficient of non-linearity of k-T curve
Γ = boundary or surface of an object
γ = Twomey regularization parameter
σ = standard deviation

Superscripts

meas = measured or specified value
comp = computed or predicted value

Subscripts

analyt = analytic
cold = cold boundary
hot = hot boundary
max = maximum value
min = minimum value
0 = reference value
1,2 = end points of an interval

References

[1] Annual Book of Standards, 1997, Section 4, Vol. 04.06, *Thermal Insulation; Environmental Acoustics*, ASTM Designation: C 177-97.

[2] Beck, J. V., Blackwell, B., and St. Clair, C. R., 1985, *Inverse Heat Conduction: III-Posed Problems*, John Wiley and Sons, New York.

[3] Alifanov, O. M., 1994, *Inverse Heat Transfer Problems*, Springer-Verlag, Berlin.

[4] Artyukhin, E. A., 1993, "Iterative Algorithms for Estimating Temperature-Dependent Thermophysical Characteristics," *Proceedings of Inverse Problems in Engineering, Theory and Practice*, N. Zabaras, et al., eds., ASME, New York, pp. 101–108.

[5] Beck, J. V., and Arnold, K. J., 1997, *Parameter Estimation in Engineering and Science*, John Wiley and Sons, New York.

[6] Orlande, H. R. B., and Ozisik, M. N., 1993, "Determination of the Reaction Function in a Reaction-Diffusion Parabolic Problem," *Inverse Problems in Engineering: Theory and Practice*, N. Zabaras et al., eds., ASME, New York, pp. 117–124.

[7] Dantas, L. B., and Orlande, H. R. B., 1996, "A Function Estimation Approach for Determining Temperature-Dependent Thermophysical Properties," Inverse Probl. Eng., **3**, No. 4, pp. 261–280.

[8] Lam, T. T., and Yeung, W. K., 1995, "Inverse Determination of Thermal Conductivity for One-Dimensional Problems," J. Thermophys. Heat Transfer, **9**, No. 2, pp. 335–344.

[9] Yang, C.-Y., 1997, "Non-Iterative Solution of Inverse Heat Conduction Problems in One Dimension," Commun. Numer. Meth. Eng., **13**, pp. 419–427.

[10] Huang, C.-H., Yan, J.-Y., and Chen, H.-T., 1995, "Function Estimation in Predicting Temperature-Dependent Thermal Conductivity Without Internal Measurements," AIAA J. Thermophys. Heat Transf., **9**, No. 4, Oct.–Dec., pp. 667–673.

[11] Sawaf, B., Ozisik, M. N., and Jarny, Y., 1995, "An Inverse Analysis to Estimate Linearly Temperature Dependent Thermal Conductivity Components and Heat Capacity of an Orthotropic Medium," Int. J. Heat Mass Transf., **38**, No. 16, pp. 3005–3010.

[12] Arpaci, V. S., 1966, *Conduction Heat Transfer*, Addison-Wesley, Reading, MA.

[13] Hansen, P. C., 1997, *Rank-Deficient and Discrete Ill-Posed Problems: Numerical Aspects of Linear Inversion*, SIAM, Philadelphia, PA.

[14] Dulikravich, G. S., and Martin, T. J., 1996, "Inverse Shape and Boundary Condition Problems and Optimization in Heat Conduction," *Advances in Numerical Heat Transfer*, W. J. Minkowycz and E. M. Sparrow, eds., Taylor & Francis, London, pp. 324–367.

[15] Martin, T. J., and Dulikravich, G. S., 1997, "Non-Iterative Inverse Determination of Temperature-Dependent Heat Conductivities," *Symposium on Inverse Design Problems in Heat Transfer and Fluid Flow*, Vol. 2, G. S. Dulikravich, and K. A. Woodbury, eds., ASME, New York, pp. 141–150.

[16] Banerjee, P. K., and Raveendra, S. T., 1981, *Boundary Element Methods in Engineering Science*, McGraw-Hill, London.

[17] Brebbia, C. A., 1978, *The Boundary Element Method for Engineers*, John Wiley and Sons, New York.

[18] Martin, T. J., and Dulikravich, G. S., 1996, "Inverse Determination of Boundary Conditions in Steady Heat Conduction with Heat Generation," ASME J. Heat Transfer, **118**, No. 3,pp. 546–554.

[19] Brebbia, C. A., and Dominguez, J., 1989, *Boundary Elements: An Introductory Course*, McGraw-Hill, New York.

[20] Tikhonov, A. N., and Arsenin, V. Y., 1977, *Solutions of Ill-Posed Problems*, V. H. Winston, Washington, DC.

[21] Golub, G. H., and Van Loan, C. F., 1996, *Matrix Computations*, 3rd Ed., Johns Hopkins Press, Baltimore, MD.

[22] Press, W. H., Teukolsky, S. A., Vetterling, W. T., and Flannery, B. P., 1986, *Numerical Recipes in FORTRAN, The Art of Scientific Computing*, 2nd Ed., Cambridge University Press, Cambridge, UK.

[23] Twomey, S., 1963, "On the Numerical Solution of Fredholm Integral Equations of the First Kind by the Inversion of the Linear System Produced by Quadrature," J. Assoc. Comput. Mach., **10**, No. 1, pp. 78–101.

[24] Barsky, B. A., 1988, *Computer Graphics and Geometric Modeling Using Beta-Splines*, Springer-Verlag, Berlin.

[25] Chapman, A. J., 1960, *Heat Transfer*, McMillan, New York.

[26] Ho, C. Y., Powell, R. W., and Liley P. E., 1974, Thermal Conductivity of the Elements: A Comprehensive Review, *Journal of Physical and Chemical Reference Data*, Vol. 3, Supplement No. 1.